Contribution ID: **840** Type: **Regular Poster**

Magnetic configuration effects on turbulence driven transport from LHD and W7X identical experiments

Thursday, 13 May 2021 18:25 (20 minutes)

Different characteristics of turbulence driven transport were found in LHD and W7X from identical experiments of ECRH plasma. The kinetic pressure was higher in W7X in the central region (ρ<~0.4) indicating that anomalous transport is lower in W7X in this region. On the other hand, the kinetic pressure is higher in LHD in outer region (ρ>~0.4) indicating that anomalous transport is lower in LHD in this region.

LHD and W7X are presently the largest two heliotron/stellarator working devices. The identical experiments were carried out using 2MW (port through power) ECRH in two different density cases of hydrogen plasma. One case was the low density case, where line averaged density ($\bar{n}_e$) was 1.5x10^{19}m^{-3}, and the other case was the high density case, where $\bar{n}_e$ was 3x10^{19}m^{-3}. In LHD, ECRH was 154GHz 2nd harmonic heating, while in W7X, 140GHz 2nd harmonic heating. In both devices, ECRH was central heating and more than 90% injection power deposited within ρ=0.2. The configurations of LHD was inwardly shifted configuration, where the magnetic axis position was 3.6m, at 2.75T. W7X was standard configuration at 2.5T.
Figure 1 shows comparison of the rotational transform (ι) and effective helical ripple (ϵ_{eff}). LHD is characterized by high ϵ_{eff} and high ι shear, while W7X is characterized by low ϵ_{eff} and low ι shear. The signs of ι shear in both devices are opposite to tokamaks. The finite ϵ_{eff} enhances neoclassical transport[1]. In $1/\nu$ collisionality regime, the neoclassical diffusivity is proportional to $\epsilon_{eff}^{1.5}$. In W7X, magnetic configuration was optimized to reduce ϵ_{eff}. Then, neoclassical diffusivity is one order magnitude lower in W7X than in LHD at ρ>~0.5 for the same collisionality[1].

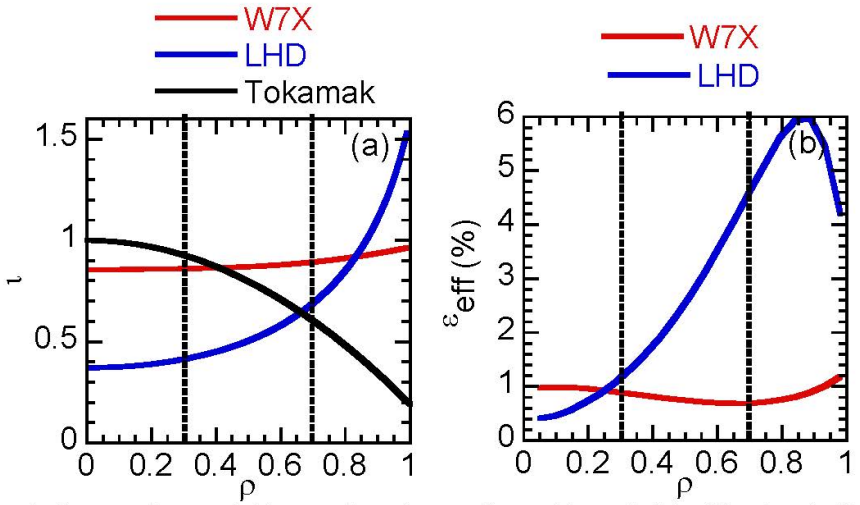

Fig.1 Comparison of (a) rotational transform (ι) and (b) effective helical ripple (ε_{eff}). ι profile in tokamak is shown as a reference. ε_{eff} is zero in tokamak. The dashed lines are ρ=0.3 and 0.7, where transport characteristics are discussed in Fig.3

Figure 1:

Figure 2 shows comparisons of profiles. As shown in Fig. 2 (d) and (h), the kinetic pressure is higher in outer region in LHD both in low and high density cases. This results in the higher kinetic stored energy and longer energy confinement time in LHD. However, central pressure is higher in W7X in both cases. Figure 3 shows a comparison of electron thermal conductivity of total values (χ_e^{total}), which consists of anomalous and neoclassical contribution, and anomalous electron thermal conductivity (χ_e^{ANO}) in low and high density

cases. In Table 1, χ_e^{total}, χ_e^{ANO} and neoclassical electron thermal conductivity (χ_e^{NEO}) at ρ=0.3 and 0.7 are summarized. In Table 1, integrated power to heat fluxe of each transport contribution is shown.

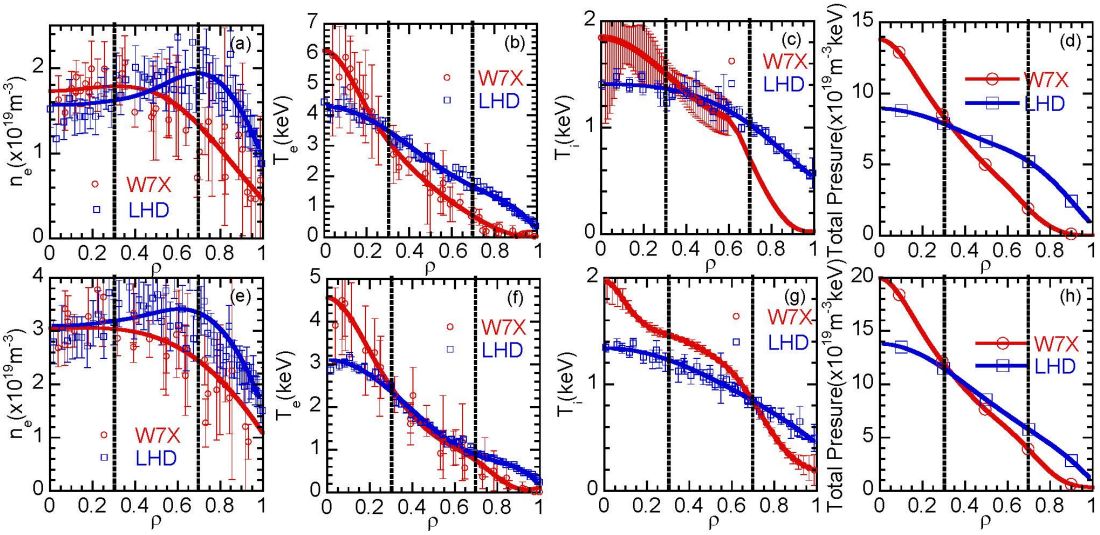

Fig. 2 Comparison of profiles (a)~(d) in low density case and (e)~(h) in high density case
The dashed lines are ρ=0.3 and 0.7, where transport characteristics are discussed in Fig.3

Figure 2:

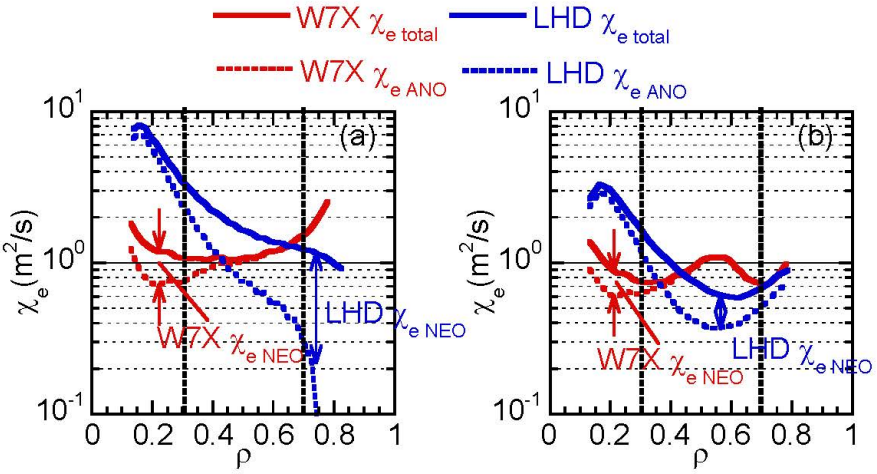

Fig.3 Electron thermal conductivity (a) in low density case and (b) in high density case.
Plain lines indicate total electron thermal conductivities.
Dashed line indicate anomalous thermal conductivities.
The differences between plain and dashed lines indicate neoclassical thermal conductivities.
Charge exchange loss and radiation loss were not included in power balance analyses, but their contributions are maximum 10% of total power.
Neoclassical coefficients are calculated by DKES and NTSS.

Figure 3:

	ρ=0.3		ρ=0.7	
	LHD	W7X	LHD	W7X
Low density $\chi_{e\ total}$ ($q_{e\ total}$)	3.5m^2/s (1.8MW)	1.1m^2/s (2.0MW)	1.2m^2/s (1.4MW)	1.6m^2/s (2.0MW)
Low density $\chi_{e\ ANO}$ ($q_{e\ ANO}$)	**2.5m^2/s (1.3MW)**	**0.8m^2/s (1.4MW)**	0.3m^2/s (0.4MW)	**1.6m^2/s (2.0MW)**
Low density $\chi_{e\ NEO}$ ($q_{e\ NEO}$)	1.0m^2/s (0.5MW)	0.3m^2/s (0.6MW)	**0.9m^2/s (0.9MW)**	- (~0MW)
High density $\chi_{e\ total}$ ($q_{e\ total}$)	1.7m^2/s (1.5MW)	0.8m^2/s (1.8MW)	0.7m^2/s (0.7MW)	0.7m^2/s (1.7MW)
High density $\chi_{e\ ANO}$ ($q_{e\ ANO}$)	**1.3m^2/s (1.1MW)**	**0.6m^2/s (1.5MW)**	**0.5m^2/s (0.6MW)**	**0.7m^2/s (1.7MW)**
High density $\chi_{e\ NEO}$ ($q_{e\ NEO}$)	0.5m^2/s (0.4MW)	0.1m^2/s (0.3MW)	0.2m^2/s (0.2MW)	- (~0MW)

Table.1 Comparison of $\chi_{e\ total}$, $\chi_{e\ ANO}$ and $\chi_{e\ NEO}$ at ρ=0.3 and 0.7
Integrated power to heat fluxes are shown in brackets.
Total integrated power (total deposition power) are 1.8MW in LHD and 2MW in W7X.
Red bold characters indicate dominant contribution.

Figure 4:

For the argument of the transport, dominant transport channel should be considered. In ECRH plasma, the external heating is only electron heating. Ion is heated by the equipartition of the energy from hot electron to cold ion. Equipartition heating (P_{ei}) is proportional to $n_e^2(T_e - T_i)$, thus, P_{ei} becomes higher at higher density. Also, contribution of neoclassical and anomalous transport should be considered as well. Configuration effects on neoclassical transport are well established[1]. However, configuration effects on anomalous transport are still under validation with theory/simulations and are absolutely essential for the design of the next generation of heliotron/stellarator devices.

In plasma central region (ρ<~0.4), electron temperature and ion temperature are clearly higher in W7X than in LHD both in low and high density cases. In central region (ρ<~0.4) of low density case, χ_e^{total} and χ_e^{ANO} are clearly lower in W7X than in LHD as shown in Fig.3 (a). As shown in Table 1, at ρ=0.3 in low density case, total electron power of 1.8MW in LHD and 2.0MW in W7X are equal to total deposition power. In low density case at ρ<~0.4, main transport is electron channel in both devices. Also, in both LHD and W7X, transport is dominated by anomalous transport, then χ_e^{ANO} becomes close to χ_e^{total} as shown in Fig.3 (a). This is due to the low ϵ_{eff} in this region in both devices as shown in Fig.1. Thus, lower χ_e^{total} and χ_e^{ANO} in W7X than in LHD is due to lower anomalous transport in W7X. In high density case of central region (ρ<~0.4), qualitative characteristics of transports are similar to low density case.

In outer region of plasma (ρ>~0.4), transport characteristics are different from central region (ρ<~0.4) in both devices. At first, density profiles are clearly different in this regiom of LHD and W7X. As shown in Fig. 2 (a) and (e), the density profiles are hollowed in LHD and peaked in W7X. Since particle source is localized in plasma edge region (ρ>~0.9), the opposite sign of density gradient in source free region (ρ<~0.9) is due to the difference of the particle transport[2]. This indicates that outward convection exists in LHD, while inward convection exists in W7X. The different density profile affects P_{ei} in particular in high density case.

In outer region (ρ>~0.4) of low density case, dominant transport channel is electron channel in both devices. In LHD, transport is governed by the neoclassical transport. For example, at ρ=0.7, anomalous electron power 0.4MW is only 30% of total electron power 1.4MW. In LHD, χ_e^{total} decreases toward the plasma edge as shown in Fig.3 (a). This reduction is mainly due to the decrease of χ_e^{ANO}, because χ_e^{NEO} is almost spatially constant. Although contribution of anomalous transport is minor in low density case at ρ>~0.4 in LHD, it contributes to the reduction of total electron transport toward the plasma edge. While in W7X, neoclassical transport is negligibly small in outer region (ρ>~0.4) in low density case as shown in Fig.3 (a). In W7X, χ_e^{ANO} increases toward the plasma edge unlike as in LHD. As shown in Fig. 1, ι and ϵ_{eff} are clearly different at ρ>~0.4. The differences of ι and ϵ_{eff} in this region possibly can cause different characteristics of neoclassical and anomalous transport.

In outer region (ρ>~0.4) of high density case in both devices, contribution of neoclassical transport becomes low. Thus, the observed difference of transport is due to the difference of anomalous transport. The particularity of the outer region (ρ>~0.4) of transport in high density case is dominant transport channel. In W7X, dominant transport channel is electron channel. However, in LHD, contributions of electron and ion channel are comparable. For example, at ρ=0.7, total electron power 0.7MW is only 40% of total deposition power of 1.8MW. As shown in Fig.3 (b),χ_e^{total} and χ_e^{ANO} in LHD is lower than χ_e^{total} ~ χ_e^{ANO} in W7X at ρ>~0.4 of high density case. Electron anomalous transport is lower in LHD than in W7X in this region. In LHD, ion transport is dominated by anomalous transport as well, and anomalous ion thermal conductivity (χ_i^{ANO}) is comparable to the χ_e^{total} ~ χ_e^{ANO} in W7X. Thus, total anomalous transport is still lower in LHD than in W7X. In outer region (ρ>~0.4), anomalous electron transport is lower in LHD than in W7X both in low and high density case. It is a strong contrast to central region (ρ<~0.4), where anomalous electron transport is clearly lower in W7X than in LHD in low and high density cases. The results suggest that physics mechanism of anomalous transport is different in central region (ρ<~0.4) and outer region (ρ>~0.4) in LHD and W7X. The former can be due to difference of the Maximum-J (J is the second invariance) property[1]. The latter can be due to the difference of density profiles. The hollowed density profiles can suppress turbulence and hollowed density profiles in LHD are due to the neoclassical thermo-diffusion[3].

1. P. Helander et al, Plasma Phys. Control. Fusion 54 (2012) 124009
2. Y. Ohtani et al, Plasma Phys. Control. Fusion 62 (2020) 025029
3. K. Tanaka et al, Plasma Phys. Control. Fusion 62 (2020) 024006

Affiliation

National Institute for Fusion Science

Country or International Organization

Japan

Primary author: TANAKA, Kenji (National Institute for Fusion Science)

Co-authors: WARMER, Felix (Max Planck Institute for Plasma Physics); NUNAMI, Masanori (National Institute for Fusion Science); Dr OHTANI, Yoshiaki (National Institutes for Quantum and Radiological Science and Technology); NAKATA, Motoki (National Institute for Fusion Science); TSUJIMURA, Toru (National Institute for Fusion Science); YOSHINUMA, Mikirou (National Institute for Fusion Science); TAKAHASHI, Hiromi (National Institute for Fusion Science); YANAI, Ryohma (National Institute for Fusion Science); SHIMOZUMA, Takashi (National Institute for Fusion Science); YOKOYAMA, MASAYUKI (National Institute for Fusion Science); SEKI, RYOSUKE (National Institute for Fusion Science); SATAKE, Shinsuke (National Institute for Fusion Science, Japan); Prof. SUGAMA, Hideo (National Institute for Fusion Science); TOKUZAWA, Tokihiko (National Institute for Fusion Science); Dr YASUHARA, Ryo (NIFS); TAKEMURA, Yuki (National Institute for Fusion Science); Dr FUNABA, Hisamichi (NIFS); Dr YAMADA, Ichihiro (NIFS); IDA, Katsumi (National Institute for Fusion Science); Prof. PETERSON, Byron (National Institute for Fusion Science); SUZUKI, Yasuhiro (National Institute for Fusion Science); KUBO, Shin (National Institute for Fusion Science); Dr SUZUKI, Chihiro (National Institute for Fusion Science); OSAKABE, Masaki (National Institute for Fusion Science); MORISAKI, Tomohiro (National Institute for Fusion Science); YAMADA, Hiroshi (The University of Tokyo); Dr XANTHOPOULOS, Pavlos (Max-Planck-Institut für Plasmaphysik Greifswald); HELANDER, Per (Max Planck Institute for Plasma Physics); Dr BEIDLER, Craig (Max-Planck-Institut für Plasmaphysik); Dr STANGE, Torsten (Max-Planck Institut für Plasmaphysik); Dr SMITH, Håkan (Max-Planck-Institut für Plasmaphysik); Dr TURKIN, Yuriy (Max-Planck Institut für Plasmaphysik); Dr BRUNNER, Kai Jakob (Max-Planck Institut für Plasmaphysik); Dr VON STECHOW, Adrian (Max-Planck-Institut für Plasmaphysik); GEIGER, Joachim (Max-Planck-Institute for Plasma Physics, Greifswald, Germany); PABLANT, Novimir (Princeton Plasma Physics Laboratory); LANGENBERG, Andreas (Max-Planck-Institut für Plasmaphysik,17491 Greifswald, Germany); Dr PASCH, Ekkehard (Max-Planck-Institute for Plasma Physics); FUCHERT, Golo (Max--Planck-Institut für Plasmaphysik, Greifswald, Germany); BOZHENKOV, Sergey (Max-Planck-Institut für Plasmaphysik, Greifswald, Germany); Dr SCOTT, Evan (Max-Planck Institut für Plasmaphysik); WOLF, Robert (Max--Planck-Institute for Plasma Physics); Dr PLUNK, Gabriel (Max-Planck-Institut für Plasmaphysik Greifswald); Dr ZHANG, Daihong (Max-Planck-Institut für Plasmaphysik Greifswald)

Presenter: TANAKA, Kenji (National Institute for Fusion Science)

Session Classification: P6 Posters 6

Track Classification: Magnetic Fusion Experiments